

## Determination of Formation and Ionization Energies of Charged Defects in Two-Dimensional Materials

Dan Wang,<sup>1</sup> Dong Han,<sup>1,2</sup> Xian-Bin Li,<sup>1,\*</sup> Sheng-Yi Xie,<sup>1</sup> Nian-Ke Chen,<sup>1</sup> Wei Quan Tian,<sup>1,3</sup> Damien West,<sup>2</sup> Hong-Bo Sun,<sup>1,†</sup> and S. B. Zhang<sup>1,2,‡</sup>

<sup>1</sup>*State Key Laboratory on Integrated Optoelectronics, College of Electronic Science and Engineering, Jilin University, Changchun 130012, China*

<sup>2</sup>*Department of Physics, Applied Physics, and Astronomy, Rensselaer Polytechnic Institute, Troy, New York 12180, USA*

<sup>3</sup>*Institute of Theoretical Chemistry, Jilin University, Changchun 130012, China*

(Received 12 September 2014; published 12 May 2015)

We present a simple and efficient approach to evaluate the formation energy and, in particular, the ionization energy (IE) of charged defects in two-dimensional (2D) systems using the supercell approximation. So far, first-principles results for such systems can scatter widely due to the divergence of the Coulomb energy with vacuum dimension, denoted here as  $L_z$ . Numerous attempts have been made in the past to fix the problem under various approximations. Here, we show that the problem can be resolved without any such assumption, and a converged IE can be obtained by an extrapolation of the asymptotic IE expression at large  $L_z$  (with a fixed lateral area  $S$ ) back to the value at  $L_z = 0$ . Application to defects in monolayer boron nitride reveal that defects in 2D systems can be unexpectedly deep, much deeper than the bulk.

DOI: 10.1103/PhysRevLett.114.196801

PACS numbers: 73.20.Hb, 68.55.Ln, 73.22.-f

Defect physics is at the heart of semiconductor physics [1], as the electronic and optoelectronic properties of a semiconductor are often determined by defects, with effects ranging from providing free carriers to acting as undesirable carrier traps and/or nonradiative recombination centers. Recently, the development of two-dimensional (2D) semiconductors such as transition metal dichalcogenides [2,3], boron nitride [3–5], and phosphorene [6–8], has attracted considerable attention. Different from their 2D predecessor, graphene, these materials all have nonzero band gaps comparable to those of ordinary semiconductors such as Si and GaAs. This has raised the expectation that one may replace traditional semiconductors by 2D materials with drastically reduced size. However, one still has to demonstrate that the defect behavior in such 2D materials is not significantly different from that of ordinary semiconductors. In particular, to apply device concepts from existing technologies, one must find adequate dopants which can be ionized near room temperature to provide the desired free carriers. This has prompted an intense study of defect properties in 2D materials including a number of first-principles calculations, for example, for monolayer BN [9,10], MoS<sub>2</sub> [11,12], GaN [13], AlN [14], GaS/GaSe [15], and SnS<sub>2</sub> [16].

The key measure of a dopant performance is its ionization energy (IE), i.e., the energy required to free electrons or holes from the dopants into the conduction or valence bands, respectively. In fact, a large number of promising wide-gap semiconductors still cannot be used for electronic applications because of the inability to achieve desired free

carrier densities by doping [1]. Calculation of the IEs relies on the ability to accurately calculate the formation energies of both neutral and charged defects. First-principles defect calculations invoke the periodic boundary conditions, which, however, introduce artificial long-range Coulomb interactions between a charged defect and its periodic images, and consequently, a divergence. This divergence is routinely removed through the use of a homogenous counter charge (i.e., the so-called jellium background) to neutralize the supercell [17]. In calculating a charged defect in a three-dimensional (3D) system, the error in the defect energy may be expressed as  $\delta E \propto 1/L$ , where  $L$  is the cube root of the supercell volume ( $L = \sqrt[3]{V}$ ) [18]. While  $\delta E \rightarrow 0$  at the zero jellium density limit, i.e.,  $L \rightarrow \infty$ , there is no simple expression so far for the proportionality constant.

For defects in a 2D system, one could, in principle, treat the system as a special case of a 3D system, as demonstrated for a model quasi-2D system in Ref. [19]. Due to the poor screening in the  $z$  direction, such an approach usually requires a very large  $L \propto \sqrt[3]{L_x L_y L_z} \propto L_z$ , in order to include a large enough empty space in the vacuum direction, often making such calculations computationally prohibitive. Instead, 2D defect calculations typically take the limit  $L_z \rightarrow \infty$  (in the vacuum direction) at a fixed lateral area  $S \propto L_x \times L_y$ . However, while in a 3D system the jellium is contained within bulk, in a 2D system it extends into vacuum and, as a consequence, the Coulomb energy of the system diverges as  $L_z \rightarrow \infty$ . A number of studies for 2D charged defects have been based on such an approach, reporting widely spread results with arbitrarily chosen  $L_z$

[9,10,13–16]. For almost two decades [20], this problem has remained unresolved, despite the importance of studying charged surface defects and catalysis involving charged species at surfaces. Methods to overcome the problem include those introducing a neutralizing charge [21–23] or fixing the potential at cell boundary [24–26]. Recently, another supercell correction method was proposed [19]. However, it depends on the construction of a model Gaussian charge, which may be good only for very localized defects, and an effective dielectric constant that depends only on  $z$ . Application to monolayer systems is an example of the limitations of the model, as a modified dielectric constant profile from the density functional perturbation theory must be adopted [11,27].

In this Letter, we propose a method for charged defects in 2D systems free of any of the above *ad hoc* assumptions and/or tunable model parameters, thereby maintaining the simplicity of the supercell approximation. A key development is the formulation of the asymptotic behavior of the defect energies at large  $L_z$  and lateral area  $S$ . Taking IE as an example, we show by first-principles methods how to calculate the converged value ( $\text{IE}_0$ ) accurately and efficiently. We also show that, for any negative-charge acceptorlike defect in a supercell with fixed  $S$ , increasing  $L_z$  always leads to the unphysical occupation of vacuum states. Although not previously discussed in the literature, this can render a 2D or quasi-2D charged defect correction scheme erroneous. Application to boron and nitrogen vacancies,  $V_B$  and  $V_N$ , and substitutional carbon,  $C_B$  and  $C_N$ , in monolayer BN reveal that the converged IEs ( $\geq 1.4$  eV) are all very deep. This results can be contrasted to those for 3D cubic BN (0.0–0.37 eV), which are considerably shallower. It raises the question whether chemical doping is a viable approach for electronic applications of 2D materials.

The calculations were performed using the density functional theory (DFT) [28,29], as implemented in the VASP codes [30,31]. Here, we used the Perdew-Burke-Ernzerhof functional [32] for exchange and correlation, but the methodology applies to any functional. The cutoff energy of the plane wave basis is 400 eV. A  $3 \times 3 \times 1$  Monkhorst-Pack mesh grid was used for  $k$ -point sampling. The dimension of the supercell is varied from 15 to 70 Å for  $L_z$  and from  $6 \times 6$  to  $9 \times 9$  unit cells for  $L_x \times L_y$ . To accommodate the computationally demanding calculations, the effects of spin polarization were excluded. The errors in the calculated lattice parameters were found to be less than 0.8%, when compared to experiment [33,34]. All atoms are relaxed until the Hellman-Feynman forces on individual atoms are less than  $0.02$  eV/Å. Under the jellium approximation, the formation energy of defect  $w$  with charge  $q$  is given by [35],

$$\begin{aligned} \Delta H_f(q, w) &= E_{\text{tot}}(q, w) - E_{\text{tot}}(\text{host}) + \sum_i n_i (E_i + \mu_i) \\ &\quad + q(\varepsilon_{\text{VBM}} + \varepsilon_F) \\ &= \Delta E_{\text{tot}}(q, w) + \sum_i n_i (E_i + \mu_i) + q(\varepsilon_{\text{VBM}} + \varepsilon_F), \end{aligned} \quad (1)$$

where  $E_{\text{tot}}(q, w)$  is the total energy of the defect supercell,  $E_{\text{tot}}(\text{host})$  is the energy of the same cell without the defect,  $\Delta E_{\text{tot}}(q, w) = E_{\text{tot}}(q, w) - E_{\text{tot}}(\text{host})$ ,  $n_i$  is the number of atoms being exchanged during the formation of the defect with the  $i$ th atomic reservoir of energy  $E_i + \mu_i$ , where  $\mu_i$  is the atomic chemical potential of an element relative to the energy in its stable form (either solid or gas),  $E_i$ , and  $\varepsilon_F$  is the Fermi energy relative to the valence band maximum,  $\varepsilon_{\text{VBM}}$ . To show the divergence problem for 2D systems, Fig. 1 compares  $\Delta H_f$  for charged  $C_B$  and  $C_N$  (namely,  $C_B^-$  and  $C_N^+$ ) in 2D and 3D BN.

The defect transition energy is defined by

$$\varepsilon(q/q') + \varepsilon_{\text{VBM}} = [\Delta E_{\text{tot}}(q, w) - \Delta E_{\text{tot}}(q', w)] / (q' - q), \quad (2)$$

where  $q$  and  $q'$  are two different charge states of the same defect. Notice that

$$\Delta H_f(q, w) = \Delta H_f(q = 0, w) + q[\varepsilon_F - \varepsilon(q/0)], \quad (3)$$

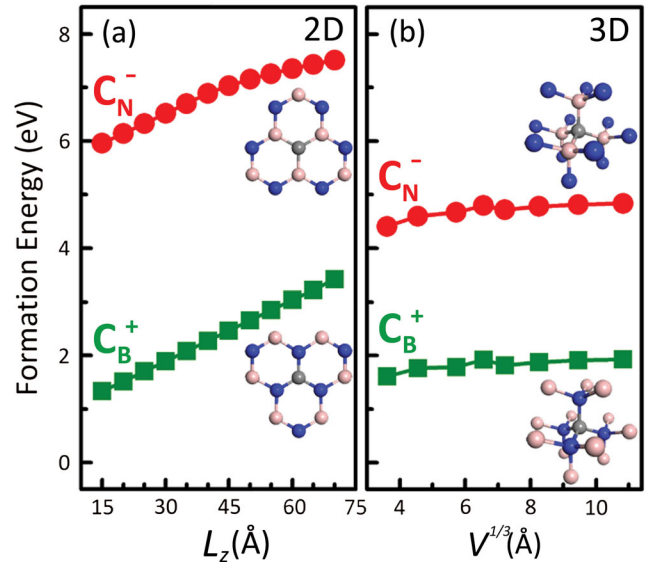


FIG. 1 (color online). Calculated formation energy of charged  $C_N^-$  and  $C_B^+$  as a function of (a) supercell size  $L_z$  (with a fixed lateral dimension:  $S$  for  $L_x \times L_y = 6 \times 6$ ) in 2D BN and (b) cube root of bulk volume in 3D BN. Insets show the local structures around the defects. Blue, pink, and gray balls are N, B, and C atoms, respectively. For bulk cubic BN, a  $3 \times 3 \times 3$  Monkhorst-Pack mesh grid was used, and the dimension of the supercell is varied from 8, 16, 32, 48, 64, 96, 144, to 216 atoms.

where the formation energy of the charge neutral defect  $\Delta H_f(q=0, w)$  can be readily calculated without any errors associated with the jellium approximation. Hence, in 2D systems, finding  $\Delta H_f(q, w)$  is equivalent to finding  $\varepsilon(q/0)$ , and the two share the same divergence. Furthermore, IEs are simply special cases of the defect transition energies,  $\varepsilon(q/q')$ , relative to the band edges. A transition of a defect from charge state (+) to (0), with respect to the conduction band minimum, defines a donor IE, and a transition from (0) to (-), with respect to the valence band maximum (VBM), defines an acceptor IE [35]. Both have well-defined physical meaning and hence, must not diverge.

The origin of this energy divergence in 2D systems can be understood using classical electrostatics. In the continuum limit of 2D charge density, the exact interactions of the periodic charged planes and their jellium background can be analytically written as the electrostatic energy per unit cell, yielding a linear divergence with respect to  $L_z$ , i.e.,  $E = \frac{q^2 L_z}{24\epsilon_0 S} = \beta \frac{L_z}{S}$ . It has been shown numerically that the above linear term dominates the  $L_z$  dependence for reasonably large  $L_z$  (see, for example, Fig. 1(a) and the discussion in the Supplemental Material [36]). Therefore, under this limit, other  $L_z$ -dependent terms such as  $L_z^{-1}$  may be neglected. Additionally, for real systems, one also needs to correct for the nonuniformity of the planar charge. Since in the correction, the charge distribution along the  $z$  direction is unchanged, this correction should thus be an  $L_z$ -independent 2D Madelung energy [37],  $\frac{\alpha}{\sqrt{S}}$ , where  $\alpha$  is a defect-specific Madelung constant. In other words, the ionization energy for the defect takes the asymptotic form

$$\text{IE}(S, L_z) = \text{IE}_0 + \frac{\alpha}{\sqrt{S}} + \left(\frac{\beta}{S}\right)L_z, \quad (4)$$

where  $\text{IE}(S, L_z)$  is a supercell-size-dependent quantity and only  $\text{IE}_0$  is the true, size-independent IE. One may also arrive at Eq. (4) from a different perspective, whereby formally expanding  $\text{IE}(L_s, L_z)$  in a power series of  $L_s (= L_x = L_y)$  and  $L_z$  and then take the physical limits:  $L_z \rightarrow \infty$  at a fixed  $L_s$ ,  $L_s \rightarrow \infty$  at a fixed  $L_z$ , and  $L_s = L_z = L \rightarrow \infty$ . The details can be found in the Supplemental Materials [36].

While Eq. (4) asserts that both donor and acceptor should have the same divergent slope  $k_M = \beta/S$ , where  $M$  stands for model, the actual DFT results appear to be at odds with the model. Figure 2 shows that for donors, namely,  $C_B^+$  and  $V_N^+$ , indeed a linear divergence of IE with respect to  $L_z$  is obtained with a slope  $k_D$ . As a matter of fact, the slope  $k_D = 0.038$  eV/Å in Fig. 2(a) agrees with the model to within three decimal points. For acceptors, namely,  $C_N^-$  and  $V_B^-$ , there is no such a clear linear dependence. Importantly, however, when  $20 \text{ \AA} \leq L_z \leq 40 \text{ \AA}$ , the expected dependence does hold, as shown in Fig. 2(b), with a slope  $k_A \cong k_D \cong k_M$ .

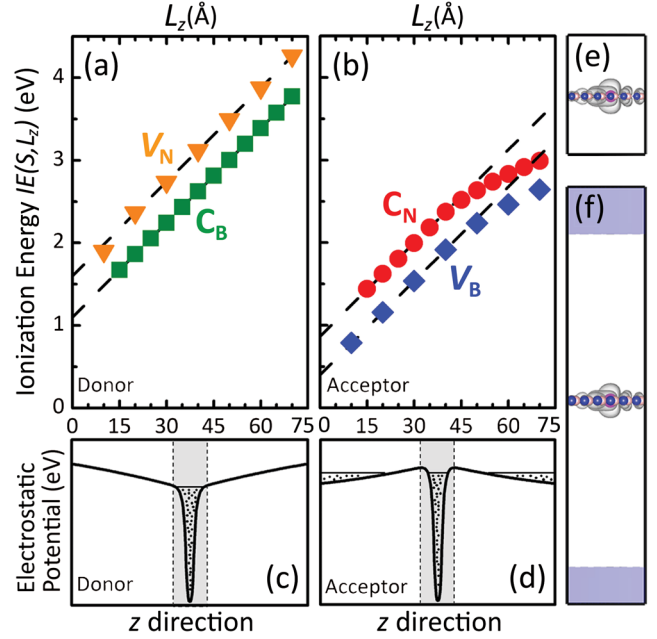


FIG. 2 (color online). Calculated IEs of (a) donors:  $C_B$  and  $V_N$ , and (b) acceptors:  $C_N$  and  $V_B$ , as a function of  $L_z$  (with a fixed lateral dimension:  $S$  for  $6 \times 6$ ). (c) and (d): schematic illustration of the corresponding electrostatic potentials. (e) and (f): acceptor state in  $C_N^-$  at different  $L_z = 20$  and  $70 \text{ \AA}$ , respectively. The shaded areas at the top and bottom of panel (f) are the calculated defect states unphysically delocalized into the vacuum. The isosurface of the electron density is  $1 \times 10^{-4}/\alpha_0^3$ , where  $\alpha_0$  is the Bohr radius.

We find that the abnormal behavior of the acceptors is a universal phenomenon, caused by the electric field inside the vacuum, due to the separation between the compensating jellium and the charged slabs. To see this, Figs. 2(c) and 2(d) compare schematically the calculated average electrostatic potentials along  $z$  for donors and acceptors, respectively: away from the 2D BN sheet, the potential for a donor increases linearly, whereas for an acceptor, it decreases linearly. Because there are (empty) electronic states in the vacuum region, a lowering of the vacuum levels relative to the occupied defect level(s) by the artificial jellium eventually leads to an unphysical occupation of the vacuum states, as can be clearly seen by the charge contour plots. For a relatively small  $L_z$ , the occupied defect charge is on the BN sheet as shown in Fig. 2(e), but for a larger  $L_z$ , the charge is also delocalized into the vacuum as shown in Fig. 2(f) (purple region in vacuum). As a result, IE starts to deviate from its linear behavior. The unphysical situation may be avoided by increasing  $S$ , which would reduce the slope of the potential in regions away from the 2D layer in Fig. 2(d) [38].

Using Eq. (4), one may obtain converged  $\text{IE}_0$  by letting  $S \rightarrow \infty$  at finite  $L_z$ . To see this, we plot  $\text{IE}(S, L_z)$  for  $V_B$ ,  $V_N$ ,  $C_B$ , and  $C_N$ , as a function of  $L_z$ . If the supercell size is large enough, according to Eq. (4), all fitted lines at different  $S$

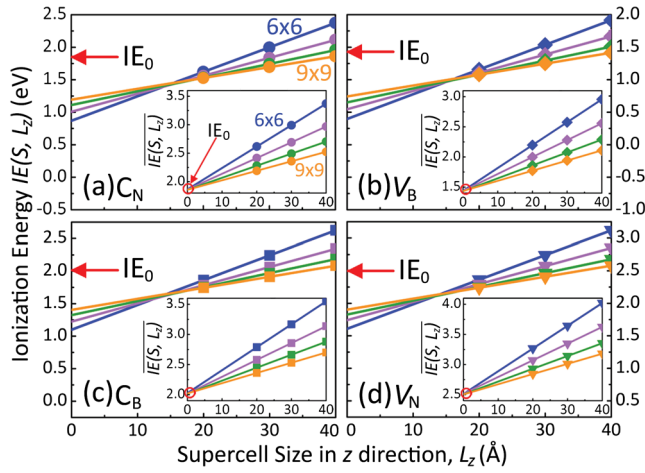


FIG. 3 (color online). Calculated IEs at different lateral dimensions ( $S$  for  $6 \times 6$ ,  $7 \times 7$ ,  $8 \times 8$ , and  $9 \times 9$ ) as a function of  $L_z$ . The insets show the value of  $\overline{\text{IE}}(S, L_z) = \text{IE}(S, L_z) - \alpha/\sqrt{S}$  as a function of  $L_z$ . The converged  $\text{IE}_0$ s (red-circle highlight) are deduced from the insets at  $L_z = 0$ .

should be linear, even though they may not intercept on the same position at  $L_z = 0$ . Figure 3 shows that indeed this is the case here. Hence, if we further define

$$\overline{\text{IE}}(S, L_z) = \text{IE}(S, L_z) - \frac{\alpha}{\sqrt{S}} = \text{IE}_0 + \left(\frac{\beta}{S}\right)L_z, \quad (5)$$

then  $\text{IE}_0$  should be the common intercept of the lines at  $L_z = 0$ , regardless of  $S$ . Note that  $\text{IE}(S \rightarrow \infty, L_z)$  also intercepts at the same point. Therefore, the difficult problem of taking the limit for  $S \rightarrow \infty$  is transformed into a simpler problem of finding an intercept at  $L_z = 0$  at finite  $S$ . Note that while we are finding the intercept of Eq. (5) for  $L_z = 0$ , this should not be confused with direct calculation of a supercell with small  $L_z$ , as Eqs. (4) and (5) are only valid for large  $L_z$ . Insets in Fig. 3 show that the  $\overline{\text{IE}}(S, L_z)$ s for  $S$  between  $6 \times 6$  and  $9 \times 9$  all intercept at a common value at  $L_z = 0$ . This is true for all the four defects being studied, demonstrating the validity of using the asymptotic form of energy [Eq. (4)] for evaluating  $\text{IE}_0$ .

Often, one needs to screen many different defects with efficiency or perform calculations using hybrid functional, with spin polarization, or spin-orbit coupling. Using the above procedure, i.e., calculating  $\alpha = \alpha_i$  for every defect  $i$  may be inefficient. Fortunately,  $\alpha$  depends primarily on the geometry of the 2D system (becoming the Madelung constant in the case of point charges), but not on the specific defect. This is illustrated in Fig. 4 where  $\text{IE}_0$ , calculated using various  $\alpha_i$ , are shown as error bars. Regardless of  $\alpha_i$  and  $S$ , the calculated  $\text{IE}_0$ s always fall onto the exact solution to within  $\pm 0.1$  eV. Hence, one only needs a one-time calculation for  $\alpha$  (using any defect) to obtain the IEs, and this can be done using even a modest  $S$  value (say the smallest  $S$  for  $6 \times 6$  in Fig. 3).

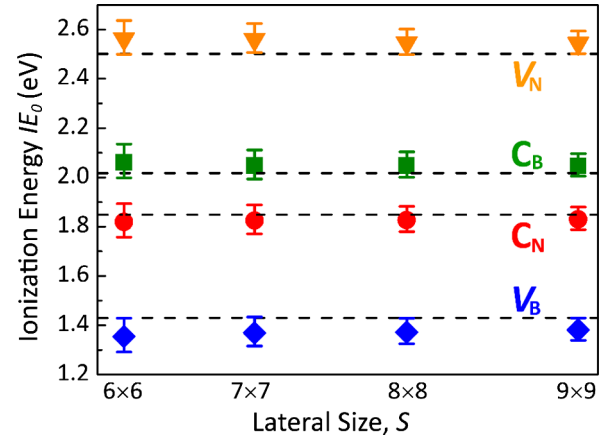


FIG. 4 (color online). Ionization energies, calculated at finite lateral dimension  $S$  with different  $\alpha_i$ , are shown as the error bars. Symbols are the averaged results. Dashed lines are the converged IEs for comparison.

The converged IEs for defects in monolayer BN are all deep, 1.86 eV for  $C_N$ , 2.03 eV for  $C_B$ , 1.44 eV for  $V_B$ , and 2.50 eV for  $V_N$ . The results for  $C_N$  and  $C_B$  may be compared to those in Ref. [27], which are 2.03 and 2.24 eV, respectively. Both methods perform well against an additional benchmark calculation we performed, in which we directly extrapolated the linear dependence in  $1/L$  of the ionization energy of the  $C_B$  defect in large supercells (ranging from  $15 \times 15$  to  $19 \times 19$ ) with  $L = L_x = L_y = L_z$ , yielding a limiting value of 2.13 eV. Our results may also be contrasted to those of cubic BN, 0.18 eV for  $C_N$ , 0.00 eV for  $C_B$ , 0.37 eV for  $V_B$ , and 0.36 eV for  $V_N$ . The results of  $V_B$  and  $V_N$  for cubic BN are in line with those in the literature [39,40]. Clearly, the ability to ionize a defect or chemical dopant in the 2D system has been drastically reduced.

In summary, we propose a simple and model-free approach to accurately and efficiently evaluate the formation energy and IE of charged defects in 2D systems. We showed that converged IE is given by the  $S \rightarrow \infty$  limit, which can be obtained by extrapolating the asymptotic function at large  $L_z$  and finite  $S$  back to the  $L_z = 0$  value. We identified the unphysical occupation of vacuum states for all acceptors when the vacuum region is sufficiently large, which puts a restriction on most charged defect correction schemes. Unlike some of the other methods that are strongly system specific, our method equally applies to quasi-2D systems such as semiconductor surfaces [19,20,41] and semiconductor-liquid interfaces [42]. Application to 1D charged systems is also straightforward by using the asymptotic expression (S9) from the Supplemental Materials [36].

The work was supported by National Natural Science Foundation of China (Grants No. 11104109, No. 11374119, No. 91423102, No. 91323301), China

Postdoctoral Science Foundation (Grant No. 2013T60315). DW and SBZ were supported by the U.S. Department of Energy (Office of Basic Energy Sciences) under Grant No. DE-SC0002623. WQT thanks support from the Open Project of State Key laboratory of Supramolecular Structure and Materials (JLU) (Project No. SKLSSM2015018). Also, we acknowledge the High Performance Computing Center (HPCC) at Jilin University for calculation resources.

\*Corresponding author.  
lixianbin@jlu.edu.cn

†Corresponding author.  
hbsun@jlu.edu.cn

‡Corresponding author.  
zhangs9@rpi.edu

- [1] S. B. Zhang, *J. Phys. Condens. Matter* **14**, R881 (2002).
- [2] Q. H. Wang, K. Kalantar-Zadeh, A. Kis, J. N. Coleman, and M. S. Strano, *Nat. Nanotechnol.* **7**, 699 (2012).
- [3] M. Xu, T. Liang, M. Shi, and H. Chen, *Chem. Rev.* **113**, 3766 (2013).
- [4] D. Pacilé, J. C. Meyer, C. O. Girit, and A. Zettl, *Appl. Phys. Lett.* **92**, 133107 (2008).
- [5] G. J. Slotman and A. Fasolino, *J. Phys. Condens. Matter* **25**, 045009 (2013).
- [6] H. Liu, A. T. Neal, Z. Zhu, Z. Luo, X. Xu, D. Tománek, and P. D. Ye, *ACS Nano* **8**, 4033 (2014).
- [7] L. Li, Y. Yu, G. J. Ye, Q. Ge, X. Ou, H. Wu, D. Feng, X. H. Chen, and Y. Zhang, *Nat. Nanotechnol.* **9**, 372 (2014).
- [8] J. Qiao, X. Kong, Z.-X. Hu, F. Yang, and W. Ji, *Nat. Commun.* **5**, 4475 (2014).
- [9] B. Huang and H. Lee, *Phys. Rev. B* **86**, 245406 (2012).
- [10] S. Okada, *Phys. Rev. B* **80**, 161404(R) (2009).
- [11] J.-Y. Noh, H. Kim, and Y.-S. Kim, *Phys. Rev. B* **89**, 205417 (2014).
- [12] A. Carvalho and A. H. Castro Neto, *Phys. Rev. B* **89**, 081406(R) (2014).
- [13] C. Xia, Y. Peng, S. Wei, and Y. Jia, *Acta Mater.* **61**, 7720 (2013).
- [14] Y. Peng, C. Xia, H. Zhang, T. Wang, S. Wei, and Y. Jia, *J. Appl. Phys.* **116**, 044306 (2014).
- [15] Y. Peng, C. Xia, H. Zhang, T. Wang, S. Wei, and Y. Jia, *Phys. Chem. Chem. Phys.* **16**, 18799 (2014).
- [16] C. Xia, Y. Peng, H. Zhang, T. Wang, S. Wei, and Y. Jia, *Phys. Chem. Chem. Phys.* **16**, 19674 (2014).
- [17] C. G. Van de Walle, P. J. H. Denteneer, Y. Bar-Yam, and S. T. Pantelides, *Phys. Rev. B* **39**, 10791 (1989).
- [18] J. Lento, J.-L. Mozos, and R. M. Nieminen, *J. Phys.: Condens. Matter* **14**, 2637 (2002).
- [19] H.-P. Komsa and A. Pasquarello, *Phys. Rev. Lett.* **110**, 095505 (2013).
- [20] S. B. Zhang and A. Zunger, *Phys. Rev. Lett.* **77**, 119 (1996).
- [21] I. Dabo, B. Kozinsky, N. E. Singh-Miller, and N. Marzari, *Phys. Rev. B* **77**, 115139 (2008).
- [22] R. Rurali, M. Palummo, and X. Cartoixa, *Phys. Rev. B* **81**, 235304 (2010).
- [23] N. A. Richter, S. Siculo, S. V. Levchenko, J. Sauer, and M. Scheffler, *Phys. Rev. Lett.* **111**, 045502 (2013).
- [24] A. Y. Lozovoi, A. Alavi, J. Kohanoff, and R. M. Lynden-Bell, *J. Chem. Phys.* **115**, 1661 (2001).
- [25] M. Otani and O. Sugino, *Phys. Rev. B* **73**, 115407 (2006).
- [26] K. T. Chan, H. Lee, and M. L. Cohen, *Phys. Rev. B* **84**, 165419 (2011).
- [27] H.-P. Komsa, N. Berseneva, A. V. Krasheninnikov, and R. M. Nieminen, *Phys. Rev. X* **4**, 031044 (2014).
- [28] P. Hohenberg and W. Kohn, *Phys. Rev.* **136**, B864 (1964).
- [29] W. Kohn and L. J. Sham, *Phys. Rev.* **140**, A1133 (1965).
- [30] G. Kresse and J. Furthmüller, *Comput. Mater. Sci.* **6**, 15 (1996).
- [31] G. Kresse and J. Furthmüller, *Phys. Rev. B* **54**, 11169 (1996).
- [32] J. P. Perdew, K. Burke, and M. Ernzerhof, *Phys. Rev. Lett.* **77**, 3865 (1996).
- [33] E. Knittle, R. M. Wentzcovitch, R. Jeanloz, and M. L. Cohen, *Nature (London)* **337**, 349 (1989).
- [34] C. Jin, F. Lin, K. Suenaga, and S. Iijima, *Phys. Rev. Lett.* **102**, 195505 (2009).
- [35] S. B. Zhang and J. E. Northrup, *Phys. Rev. Lett.* **67**, 2339 (1991).
- [36] See Supplemental Materials at <http://link.aps.org/supplemental/10.1103/PhysRevLett.114.196801> for derivation of the asymptotic behavior of  $\text{IE}(L_s, L_z)$ .
- [37] P. C. N. Pereira and S. W. S. Apolinario, *Phys. Rev. E* **86**, 046702 (2012).
- [38] In cases when a small  $S$  is unavoidable, this unphysical situation may be avoided by adding an *ad hoc* repulsive potential to the vacuum region. The contribution of the potential to the total energy, however, have to be removed.
- [39] W. Orellana and H. Chacham, *Phys. Rev. B* **63**, 125205 (2001).
- [40] F. Tian, Z. Liu, Y. Ma, T. Cui, B. Liu, and G. Zou, *Solid State Commun.* **143**, 532 (2007).
- [41] P. Ebert, *Surf. Sci. Rep.* **33**, 121 (1999).
- [42] A. L. Linsebigler, G. Lu, and J. T. Yates, *Chem. Rev.* **95**, 735 (1995).